Penerbit UTHM

IJIE
http://penerbit.uthm.edu.my/ojs/index.php/ijie
ISSN : 2229-838X e-ISSN : 2600-7916

The International Journal of Integrated Engineering

Correlation Between Cutting Force and Residual Stress in Dry End-Milling of Inconel HX

Mohd Nor N. A.[1*], Baharudin B. T. H. T.[2], Leman Z.[2], Mohd Ariffin M. K. A.[2]

[1]Technology and Technical Accreditation Secretariat,
Malaysia Board of Technologists, 62250 Putrajaya, MALAYSIA

[2]Department of Mechanical and Manufacturing Engineering, Faculty of Engineering,
Universiti Putra Malaysia, 43400 Serdang, MALAYSIA

*Corresponding Author

DOI: https://doi.org/10.30880/ijie.2022.14.06.005
Received 31 January 2021; Accepted 14 August 2021; Available online 10 November 2022

Abstract: Residual stress in the end-milled subsurface can significantly affect the fatigue performance of end-milled material. In the end-milling process, the generation of residual stress is extremely complex, which is closely related to the spindle speed, feed per tooth and cutting force. Thus, it is crucial to elucidate the influence of spindle speed and feed per tooth on cutting force and residual stress, also the correlation between cutting force and residual stress in terms of spindle speed and feed per tooth. According to this, dry end-milling of Inconel HX was performed by climb-milling using Kennametal KYS40 solid ceramic end-mill. From this experimental test, cutting force and residual stress showed a U-shaped relationship with the increase of spindle speed, while cutting force and residual stress showed a linear relationship with the increase of feed per tooth. Furthermore, for low cutting force and residual stress, the focus should be on choosing the optimum combination of spindle speed (21,400 to 24,100 rpm) and feed per tooth (0.014 to 0.016 mm/tooth).

Keywords: Spindle speed, feed per tooth, dry end-milling, cutting force, residual stress

1. Introduction

Residual stress refers to an internal stress distribution that remains in a material, and this stress is generated after the material experiences plastic deformation caused by mechanical load or/and thermal load [1]. In view of the machining process, residual stress presents a challenge to production sectors due to the small changes in this stress can have a significant effect on the fatigue performance of machined material [2, 3]. Harmful residual stress can lead to deformation, cracks formation and other defects [4]. Machining strategy can be applied to characterize as well as to obtain favorable residual stress for improvement on fatigue performance of machined material [3]. Apart from machining strategy, residual stress can be categorized into two; compressive residual stress and tensile residual stress. Residual stress with incremental decrease in magnitude is classified as compressive residual stress, while residual stress with incremental increase in magnitude is classified as tensile residual stress [5]. Moreover, high fatigue strength is associated with the presence of compressive residual stress, while low fatigue strength is associated with the presence of tensile residual stress [6]. Masmiati et al. (2016) and Thakur and Gangopadhyay (2016) indicated that the changes from compressive residual stress to tensile residual stress, and vice versa is strongly influenced by machining parameter. Due to this, machining strategy has attracted great attention from metal cutting researchers to exploit residual stress changes for improvements on fatigue performance of machined material.

Machining parameter consists of cutting speed, feed rate and depth of cut. These three parameters are closely related to cutting force. Cutting force decreases with increase in cutting speed [5], in contrast, cutting force decreases

*Corresponding author: noraznan.namn@gmail.com

with decrease in feed rate [8] and depth of cut [9]. On another note, residual stress is directly proportional to cutting force [10]. Excessive cutting force can cause low machined surface quality [9], chatter [11], short cutting tool life [12], etc. End-milling process is one of the commonly machining processes used in the production sector to produce aerospace components [13, 14]. In view of the end-milling, cutting speed is tied to spindle speed, whereas feed rate is tied to spindle speed and feed per tooth. Decrease in feed per tooth will decrease feed rate, however, increase in spindle speed will not only increase cutting speed but increase feed rate too. Due to this complexity, it is very difficult to understand the influence of spindle speed and feed per tooth on cutting force and residual stress, as well as the correlation between cutting force and residual stress in the aspect of spindle speed and feed per tooth. Hence, selection of spindle speed and feed per tooth combination for obtaining low cutting force and residual stress before performing end-milling process becomes complicated.

In this manuscript, end-milling test is experimentally performed to elucidate the influence of spindle speed and feed per tooth on cutting force and residual stress. It is also done to determine the correlation between cutting force and residual stress in the aspect of spindle speed and feed per tooth. Inconel HX is selected as experimental specimen since it is widely used as a material for gas turbine engine components. In addition, this nickel-based superalloys possess great mechanical properties; outstanding oxidation resistance [15] and high-strength at elevated temperatures [16]. Furthermore, KSY40 Kennametal solid ceramic end-mill is selected as experimental cutting tool in order to match with great mechanical properties of Inconel HX, and also due to the end-milling test is performed under environmentally friendly dry cutting conditions. Additionally, solid ceramic end-mill is rarely used and researched due to the aspect of design and manufacturing restrictions [17, 18]. The most important outcome from this research is to propose the range of optimum combination of spindle speed and feed per tooth for low cutting force and residual stress. Most of the optimum machining parameters from previous research is proposed in specific value, thus it becomes too rigid compared to range. By using this range, will enable production sector to select the appropriate spindle speed value and feed per tooth value based on their milling machine capacity.

2. Experimental Procedure

In this experimental test, dry end-milling of Inconel HX was carried out on a Mori Seiki NV 4000 DCG vertical machining centre with a capacity of 13 drive power rating and 45 Nm torque. The Inconel HX specimen was untreated with original hardness 92 HR_B, with dimension of 90 × 40 × 10 mm. Climb-milling was performed using KYS40 Kennametal 6 mm solid ceramic 4 flutes end-mill. Figure 1 presents the Inconel HX specimen and KYS40 Kennametal 6 mm solid ceramic 4 flutes end-mill, while Table 1 depicts the factors and levels used in the experimental test.

(a) **(b)**

Fig. 1 - Specimen and cutting tool (a) Inconel HX; (b) KYS40 Kennametal solid ceramic end-mill

Table 1 - Factors and levels used in the experimental test

Factor	Level
Spindle speed (rpm)	21,400, 24,100 and 26,800
Feed per tooth (mm/tooth)	0.013, 0.016 and 0.019
Axial depth of cut (mm)	0.2
Radial depth of cut (mm)	6

Furthermore, new end-mill was used for each test with the cutting length set at 24 mm per test. As illustrated in Figure 2, Kistler 9129AA dynamometer was used to record cutting force components; feed force (F_x), normal force (F_y) and axial force (F_z).

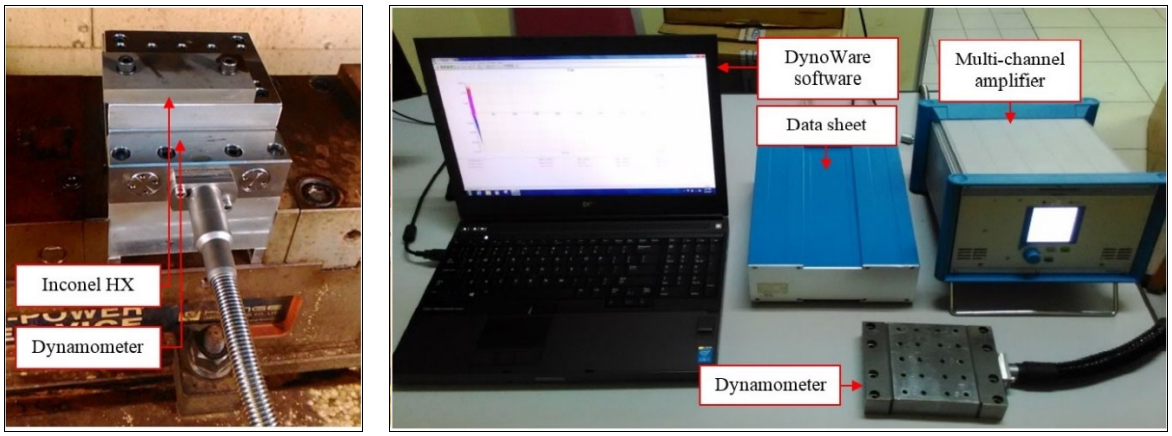

(a) **(b)**

Fig. 2 - Specimen and dynamometer (a) Inconel HX and Kistler 9129AA dynamometer; (b) Kistler 9129AA dynamometer measuring chain

From the recorded F_x, F_y and F_z, resultant force (F_r) or cutting force was computed using the equation below [19].

$$F_r = \sqrt{F_x^{\,2} + F_y^{\,2} + F_z^{\,2}} \qquad (1)$$

Next, wire electrical discharge machining was performed to cut out a small rectangular piece from the cutting force specimen, as depicted in Figure 3. In addition, the small rectangular piece was used as a residual stress specimen with the dimension of 10 × 4 × 3 mm.

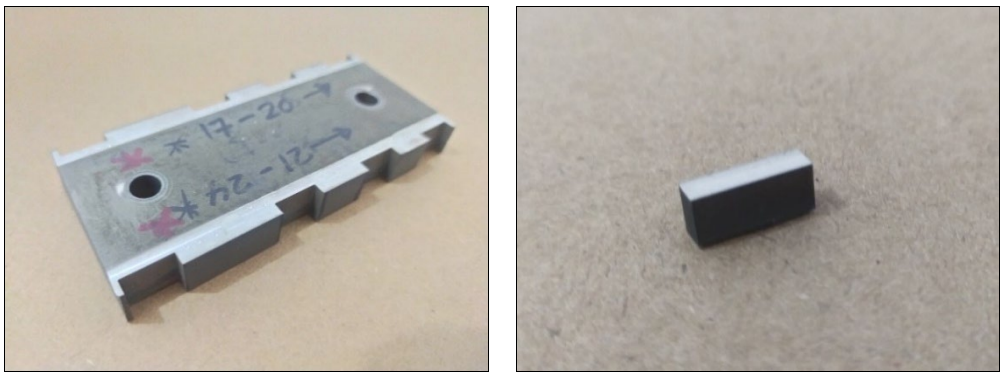

(a) **(b)**

Fig. 3 - Inconel HX (a) cutting force specimen; (b) residual stress specimen

Inconel HX residual stress was measured at the end-milled subsurface using PANalytical X'Pert Pro MPD PW 3040-60. Cu Kα was used as x-ray radiation and the tilt angle step size was set at 0.001. Space lattice was measured at five different tilt angles (ψ) and the equation below [20] was used to compute the residual stress.

$$\sigma = \left(\frac{E}{1+v}\right) m \qquad (2)$$

Where, σ is the residual stress, E is the Young's modulus, v is the Poisson's ratio, and m is the slope of space lattice against $\sin^2 \psi$. Additionally, the values of the E and v are 205 GPa [16] and 0.3 [21].

Surface plot, optimization plot and contour plot in Minitab software were applied to interpret the computed cutting force and residual stress.

3. Results and Discussion

The influence of spindle speed and feed per tooth on cutting force and residual stress, and also the correlation between cutting force and residual stress in dry end-milling of Inconel HX were interpreted using surface plot. Figure 4 and Figure 5 illustrate the computed cutting force and residual stress that are interpreted using surface plot. The meshes for the x-axis (spindle speed) and y-axis (feed per tooth) were 13 and 7, respectively. Therefore, the increment of spindle speed was 450 rpm, while the increment of feed per tooth was 0.001 mm/tooth.

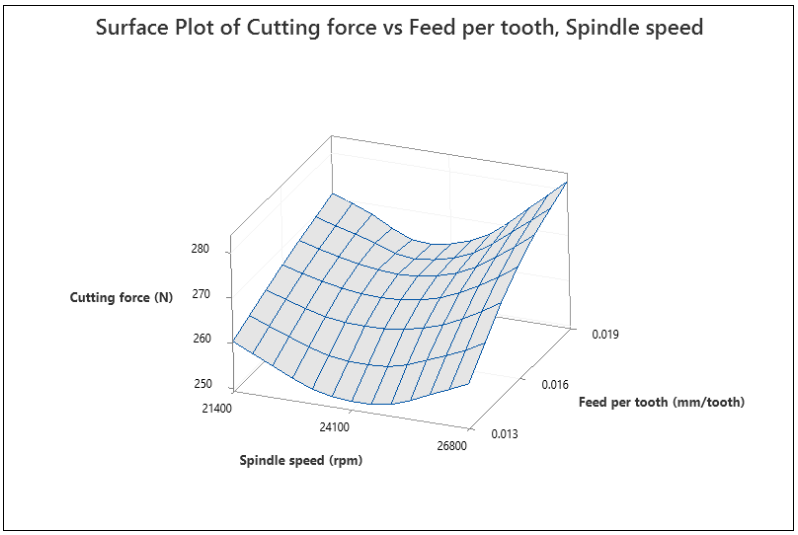

Fig. 4 - Surface plot of cutting force against feed per tooth, spindle speed

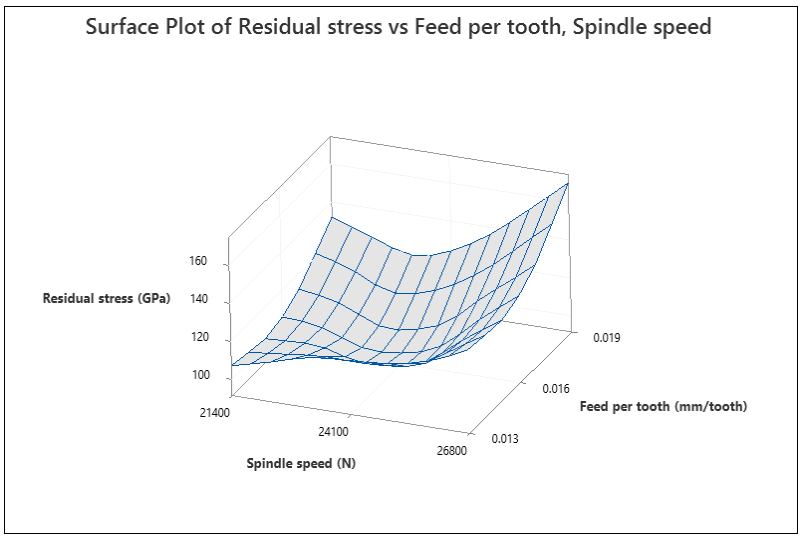

Fig. 5 - Surface plot of residual stress against feed per tooth, spindle speed

It is evident from Figure 4 that the cutting force decreases with the increase in spindle speed, but further increase in spindle speed causes an increase in cutting force. When the spindle speed is in the range of 21,400 to 24,100 rpm, the cutting force decreases, whereas it begins to increase when the spindle speed ranges from 24,100 to 26,800 rpm. This phenomenon might be associated with ductile-to-brittle transition and in agreement with the result of previous research by Mohd Nor et al. (2020). This is also supported by Wang et al. (2015), where they claimed that the machined material experiences plastic deformation at critical cutting speed during the transition from ductile regime to brittle regime, which subsequently leads to a decrease in cutting force then increases after reaching a minimum cutting force value. On

the contrary, since spindle speed is tied to cutting speed, this indicates that the experimental results contradict the theory of cutting force being inversely proportional to cutting speed as stated in the [24, 25]. As expected, cutting force has linear relationship with feed per tooth. By observing Figure 4, increasing the feed per tooth from 0.013 to 0.019 mm/tooth has led to the linearly increasing of the cutting force. The observed increase in cutting force with the increasing of feed per tooth can be attributed to the probable increase in a shear amount of unwanted Inconel HX at the solid ceramic end-mill edge [9, 26].

By comparing both surface plots in Figure 4 and Figure 5, the behavior of cutting force and residual stress showed a slight difference but similar tendency. This mismatch might be associated with uncontrolled parameters, e.g. defect of cutting force specimen during space lattice measurement. It can be proposed that there is a correlation between cutting force and residual stress in terms of spindle speed and feed per tooth. This correlation is in agreement with G. De Paula Oliveira et al. (2018) and Jiang et al. (2016), where they claimed that the residual stress strongly depends on the cutting force. Therefore, as spindle speed increases from 21,400 to 24,100 rpm, the cutting force decreases and indirectly evolves the residual stress from tensile residual stress to compressive residual stress, but further increase in spindle speed higher than 24,100 rpm causes an increase in cutting force and indirectly evolves the residual stress from compressive residual stress to tensile residual stress. Since compressive residual stress is beneficial as it tends to improve fatigue performance of machined material [6, 28], thus increasing spindle speed higher than 24,100 rpm is undesirable in dry end-milling of Inconel HX. Furthermore, variations in feed per tooth increase the residual stress where its value produced is directly proportional to the cutting force. Thus, as the feed per tooth increases, the cutting force increases, compromising the fatigue performance of Inconel HX.

In search of optimization in cutting force and residual stress, the research interest is to determine the combination of spindle speed and feed per tooth that leads to low cutting force and residual stress. The suggested combination of spindle speed and feed per tooth was obtained after analyzing the optimization plot as depicted in Figure 6.

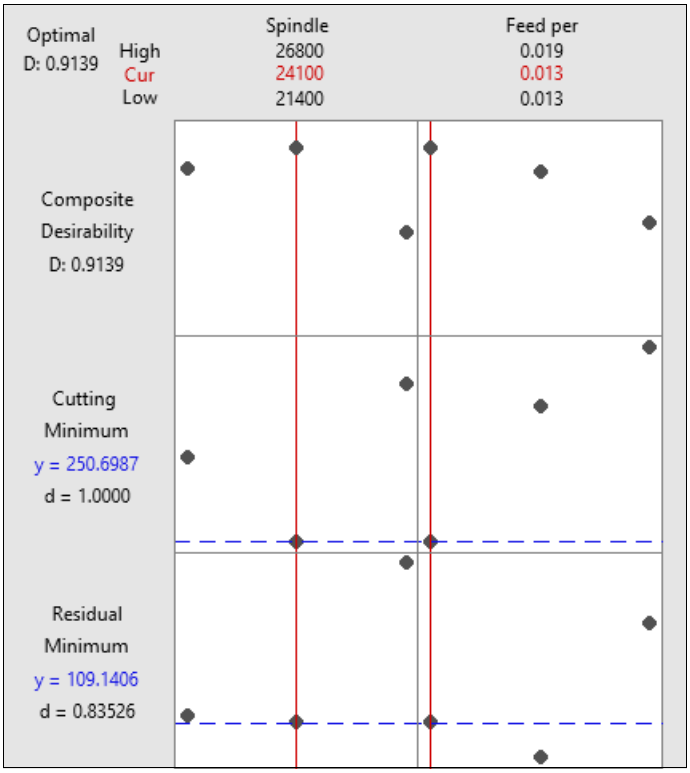

Fig. 6 - Optimization plot

Apart from this, the highest value of composite desirability or D-value indicates the combination of spindle speed and feed per tooth which corresponds with the lowest combination of cutting force and residual stress. Using the results presented in Figure 6, this combination can be obtained at a spindle speed of 24,100 rpm and accompanied with a feed per tooth at 0.013 mm/tooth which produces the highest value of composite desirability at 0.9139. However, this optimum machining parameter is too rigid; it may cause difficulty for production sectors to perform dry end-milling of Inconel HX if milling machine with a capacity of spindle speed 24,100 rpm is not available. Therefore, range is the ideal method for determining optimum machining parameter. The overall composite desirability value with individual desirability value (d-value) are extracted from Figure 6 and tabulated in Table 2.

Table 2 - Overall composite desirability value with individual desirability value

Spindle speed (rpm)	Feed per tooth (mm/tooth)	Individual desirability, d		Composite desirability, D
		Cutting force	Residual stress	
21,400	0.013	0.8052	0.8158	0.8105
24,100	0.013	1.0000	0.8353	0.9139
26,800	0.013	0.6141	0.3706	0.4771
21,400	0.016	0.4566	0.9175	0.6472
24,100	0.016	0.6718	0.9370	0.7934
26,800	0.016	0.2655	0.4723	0.3541
21,400	0.019	0.3056	0.5243	0.4003
24,100	0.019	0.5209	0.5438	0.5322
26,800	0.019	0.1145	0.0791	0.0952

By observing the results in Table 2, a spindle speed of 24,100 rpm at each level of feed per tooth had a high composite desirability value as compared with spindle speed at 21,400 and 26,800 rpm. The cutting force and residual stress recorded were 251 N and 120 GPa for spindle speed at 24,100 rpm and feed per tooth at 0.013 mm/tooth, 263 N and 97 GPa for spindle speed at 24,100 rpm and feed per tooth at 0.016 mm/tooth, and 264 N and 124 GPa for spindle speed at 24,100 rpm and feed per tooth at 0.019 mm/tooth.

The range of spindle speed and feed per tooth that leads to low cutting force and residual stress can be understood more by analyzing contour plot of composite desirability against feed per tooth, and spindle speed produced based on Table 2 as illustrated in Figure 7.

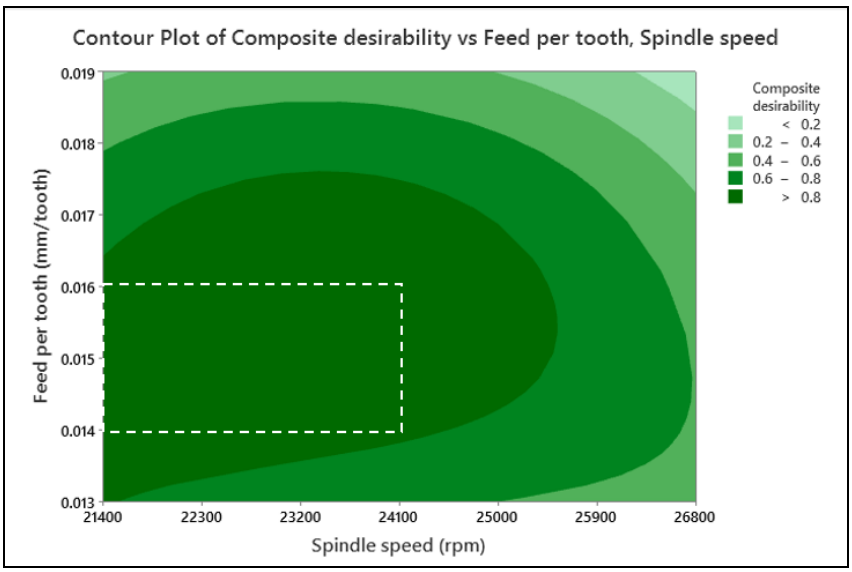

Fig. 7 - Contour plot of composite desirability against feed per tooth, spindle speed

From the contour plot, the upper right corner of the contour plot indicates the lowest composite desirability value or having a composite desirability value of 0.2 or less, which corresponds with high values of both spindle speed and feed per tooth. Whereas, darker region indicates the highest composite desirability value or having a composite desirability value of 0.8 or more. Since increasing the spindle speed higher than 24,100 rpm is undesirable, dotted rectangular box is used to set the upper and lower values of the optimum machining parameter. By referring to the dotted rectangular box in the darker region, it can be observed that the optimum combination of spindle speed and feed per tooth for low cutting force and residual stress lies in the range 21,400 to 24,100 rpm and 0.014 to 0.016 mm/tooth. Therefore, the spindle speed ranging from 21,400 to 24,100 rpm and feed per tooth ranging from 0.014 to 0.016 mm/tooth are to be chosen in achieving the optimum combination of low cutting force and residual stress during dry end-milling of Inconel HX.

4. Conclusion

Dry end-milling of Inconel HX was performed by climb-milling using Kennametal KYS40 solid ceramic end-mill. The following conclusions can be drawn from this experimental test:

- As spindle speed increases, the cutting force decreases and indirectly decreases residual stress, but further increase in spindle speed causes an increase in cutting force and indirectly increases residual stress.
- Increase in feed per tooth indirectly increases cutting force, and subsequently increases residual stress.
- The optimum combination of spindle speed and feed per tooth for low cutting force and residual stress lies in the range of 21,400 to 24,100 rpm and 0.014 to 0.016 mm/tooth. Nevertheless, the lowest combination of cutting force and residual stress can be obtained at a spindle speed of 24,100 rpm and accompanied with a feed per tooth of 0.013 mm/tooth.
- Further research should be focused on the life span of Kennametal KYS40 solid ceramic end-mill based on the proposed combination of spindle speed and feed per tooth.

Acknowledgement

This research was supported by grant No. GP-IPS/2017/9539900 from the Universiti Putra Malaysia. The authors express their sincere thanks to Mr. Mohd Nor Bin Puteh, Mdm. Hatijah Binti Kassim, Ts. Dyg. Siti Quraisyah Bt. Abg. Adenan and Mr. Nor Iman Ziqri Bin Nor Aznan.

References

[1] Gautam, N., S, AK., & Mondi, PR., (2020). Evaluation methods for residual stress measurement in large components. Materials Today: Proceedings.
[2] Wan, M., Ye, XY., Yang, Y., & Zhang, WH., (2017). Theoretical prediction of machining-induced residual stresses in three-dimensional oblique milling processes. International Journal of Mechanical Sciences, 133, 426–437.
[3] Reimer, A., & Luo, X., (2018). Prediction of residual stress in precision milling of AISI H13 steel. Procedia CIRP, 71, 329–334.
[4] Wang, C., Yu, X., Jiang, M., Xing, Z., & Wang, C., (2021). Numerical and experimental investigation into the evolution and distribution of residual stress in laser transmission welding of PC/Cu/PC. Optics & Laser Technology, 136, 106786.
[5] Masmiati, N., Sarhan, AAD., Hassan, MAN., & Hamdi, M., (2016). Optimization of cutting conditions for minimum residual stress, cutting force and surface roughness in end milling of S50C medium carbon steel. Measurement: Journal of the International Measurement Confederation, 86, 253–265.
[6] Huang, W., Zhao, J., Niu, J., Wang, G., & Cheng, R., (2018). Comparison in surface integrity and fatigue performance for hardened steel ball-end milled with different milling speeds. Procedia CIRP, 71, 267–271.
[7] Thakur, A., & Gangopadhyay, S., (2016). State-of-the-art in surface integrity in machining of nickel-based super alloys. International Journal of Machine Tools and Manufacture, 100, 25–54.
[8] Chandra, P., Rao, CRP., Kiran, R., & Kumar, VR., (2018). Influence of machining parameter on cutting force and surface roughness while turning alloy steel. Materials Today: Proceedings, 5, 11794–11801.
[9] Bolar, G., Das, A., & Joshi, SN., (2017). Measurement and analysis of cutting force and product surface quality during end-milling of thin-wall components. Measurement: Journal of the International Measurement Confederation, 121, 190–204.
[10] De Paula Oliveira, G., Fonseca, MC., & Araujo, AC., (2018). Residual stresses and cutting forces in cryogenic milling of Inconel 718. Procedia CIRP, 77, 211–214.
[11] Grossi, N., Sallese, L., Scippa, A., & Campatelli, G., (2015). Speed-varying cutting force coefficient identification in milling. Precision Engineering, 4, 321–334.
[12] Karpuschewski, B., Kundrák, J., Varga, G., Deszpoth, I., & Borysenko, D., (2018). Determination of specific cutting force components and exponents when applying high feed rates. Procedia CIRP, 77, 30–33.
[13] Cui, D., Zhang, D., Wu, B., & Luo, M., (2017). An investigation of tool temperature in end milling considering the flank wear effect. International Journal of Mechanical Sciences, 131–132, 613–624.
[14] Zhou, L., Li, J., Li, F., Mendis, G., & Sutherland, JW., (2018). Optimization parameters for energy efficiency in end milling. Procedia CIRP, 69, 312–317.
[15] Esmaeilzadeh, M., Qods, F., Arabi, H., & Sadeghi, BM., (2017). An investigation on crack growth rate of fatigue and induction heating thermo-mechanical fatigue (TMF) in Hastelloy X superalloy via LEFM, EPFM and integration models. International Journal of Fatigue, 97, 135–149.
[16] Chennamsetty, ARK., LeBlanc, J., Abotula, S., Parrikar, PN., & Shukla, A., (2016). Dynamic response of Hastelloy® X plates under oblique shocks: Experimental and numerical studies. International Journal of Impact Engineering, 92, 75–88.
[17] Wang, B., & Liu, Z., (2016). Cutting performance of solid ceramic end milling tools in machining hardened AISI H13 steel. International Journal of Refractory Metals and Hard Materials, 55, 24–32.

[18] Grguraš, D., Kern, M., & Pušavec, F., (2018). Suitability of the full body ceramic end milling tools for high speed machining of nickel based alloy Inconel 718. Procedia CIRP, 77, 630–633.
[19] Shixiong, W., Wei, M., Bin, L., & Chengyong, W., (2016). Trochoidal machining for the high-speed milling of pockets. Journal of Materials Processing Technology, 233, 29–43.
[20] Jafarian, F., Amirabadi, H., & Sadri, J., (2015). Experimental measurement and optimization of tensile residual stress in turning process of Inconel 718 superalloy. Measurement, 63, 1–10.
[21] Berke, RB., Sebastian, CM., Chona, R., Patterson, EA., & Lambros, J., (2016). High temperature vibratory response of Hastelloy-X: Stereo-DIC measurements and image decomposition analysis. Experimental Mechanics, 56, 231–243.
[22] Mohd Nor, NA., Baharudin, BTHT., A Ghani, J., Leman, Z., & Mohd Ariffin, MKA., (2020). Effect of chip load and spindle speed on cutting force of Hastelloy X. Journal of Mechanical Engineering and Sciences, 14, 6497 - 6503.
[23] Wang, B., Liu, Z., Su, G., Song, Q., & Ai, X., (2015). Investigations of critical cutting speed and ductile-to-brittle transition mechanism for workpiece material in ultra-high speed machining. International Journal of Mechanical Sciences, 104, 44–59.
[24] Brinksmeier, E., Preuss, W., Riemer, O., & Rentsch, R., (2017) Cutting forces, tool wear and surface finish in high speed diamond machining. Precision Engineering, 49, 293–304.
[25] Kadam, GS., & Pawade, RS., (2017). Surface integrity and sustainability assessment in high-speed machining of Inconel 718 – An eco-friendly green approach. Journal of Cleaner Production, 147, 273–283.
[26] Gaikhe, V., Sahu, J., & Pawade, R., (2018). Optimization of cutting parameters for cutting force minimization in helical ball end milling of Inconel 718 by using genetic algorithm. Procedia CIRP, 77, 477–480.
[27] Jiang, X., Li, B., Wang, L., Wang, Z., & Li, H., (2016). An approach to evaluate the effect of cutting force and temperature on the residual stress generation during milling. The International Journal of Advanced Manufacturing Technology, 87, 2305–2317.
[28] Tan, L., Zhang, D., Yao, C., Wu, D., & Zhang, J., (2017). Evolution and empirical modeling of compressive residual stress profile after milling, polishing and shot peening for TC17 alloy. Journal of Manufacturing Processes, 26, 155–165.